



Original Article

Comparison of intestinal absorption characteristics between rhubarb traditional Chinese medicine preparation and activity ingredients using *in situ* and *in vitro* model

Wenjing Ta^a, Xiaoying Yang^b, Jie Wang^a, Chengkun Han^a, Ruochen Hua^a, Wen Lu^{a,*}

^a Health Science Center, School of Pharmacy, Xi'an Jiaotong University, Xi'an 710061, China

^b Shaanxi Regional Center, National Anti-Drug Laboratory, Xi'an 710000, China

ARTICLE INFO

Article history:

Received 4 January 2022

Revised 8 April 2022

Accepted 19 September 2022

Available online 5 December 2022

Keywords:

absorption characteristics
Caco-2 cell monolayer model
rhubarb anthraquinone
single-pass intestinal perfusion model
traditional Chinese medicine

ABSTRACT

Objective: The intestinal absorption characteristics of active ingredients are very important for oral administration of traditional Chinese medicine (TCM) to achieve the desired therapeutic effect. However, a deeper understanding about active ingredients absorption characteristics is still lack. The aim of this study was to investigate the absorption properties and mechanism of rhubarb active ingredients in TCM preparation and pure form.

Methods: The intestinal absorption behavior of active ingredients in Shenkang extract (SKE) and rhubarb anthraquinone ingredients (RAI) were investigated by *in situ* single-pass intestinal perfusion model. And the bidirectional transport characteristics of these active ingredients were assessed by *in vitro* Caco-2 cell monolayer model.

Results: *In situ* experiment on Sprague-Dawley rats, the effective permeability coefficient values of aloemodin, emodin and chrysophanol in RAI were higher than those in SKE, and the value of rhein in RAI was lower than that in SKE. But the easily absorbed segments of intestine were consistent for all ingredients, whether in SKE or in RAI. *In vitro* experiment, the apparent permeability coefficient values of rhein, emodin and chrysophanol in RAI were higher than those in SKE, and this value of aloemodin in RAI was lower than that in SKE. But their efflux ratio (ER) values in SKE and RAI were all similar.

Conclusion: Four rhubarb anthraquinone ingredients in SKE and RAI have similar absorption mechanism and different absorption behavior, and the microenvironment of the study models influenced their absorption behavior. The results may provide an aid for understanding of the absorption characteristics of the TCM active ingredients in complex environments and the complementarities of different research models.

© 2022 Tianjin Press of Chinese Herbal Medicines. Published by ELSEVIER B.V. This is an open access article under the CC BY-NC-ND license (<http://creativecommons.org/licenses/by-nc-nd/4.0/>).

1. Introduction

Traditional Chinese medicine (TCM) and multi-herb prescription have been widely used in China. Shenkang Injection, *Rhei Radix et Rhizoma* (Dahuang in Chinese) combined with *Salviae Miltiorrhizae Radix et Rhizoma* (Danshen in Chinese), *Carthami Flos* (Honghua in Chinese), and *Astragali Radix* (Huangqi in Chinese), is a marketed multi-herb prescription used for therapy chronic renal failure (Lian, Han, Fang, Li, & Zuo, 2015; Zhang, Sun, Liu, & Zhai, 2017). However, for chronic patients on long-term medication, convenient oral preparations are one of the desirable options. It is well known that many physiological and pharmaceutical factors

can affect intestinal absorption of oral formulations, resulting in low bioavailability. Therefore, it is very necessary to understand the absorption characteristics of drugs in oral preparations. Among the TCM constitute of Shenkang Injection, *Rhei Radix et Rhizoma* plays an important role and is believed to be most effective in treating the main syndrome of diseases. Rhubarb anthraquinone compounds, such as aloemodin, rhein, emodin and chrysophanol (Fig. 1), were the main characteristic active ingredients in *Rhei Radix et Rhizoma* to exert therapeutic effects (Zhang et al, 2016, 2018). There are several studies that have shown the absorption characteristics of aloemodin, emodin, rhein and chrysophanol (Zeng et al., 2017; Ying, Min, Chong, Meng, & Xiao, 2018; Yang et al., 2020). However, the differences of absorption properties of rhubarb active ingredients in TCM preparations and their pure forms remain unknown.

* Corresponding author.

E-mail address: lvlu2004@xjtu.edu.cn (W. Lu).

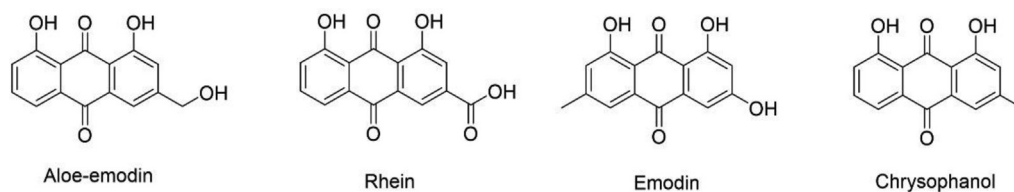


Fig. 1. Chemical structures of four rhabarb anthraquinone compounds.

To elucidate the intestinal absorption characteristics of rhabarb TCM preparation and rhabarb active ingredients, *in situ* and *in vitro* models were used to compare their absorption behaviors. The single-pass intestinal perfusion model is an important and common *in situ* absorption model, not only the microenvironment in the intestinal segments is more closely replicated, but also it can exhibit the effect of mesenteric blood flow (Lin et al., 2015). Caco-2 cell monolayer model has become a classical *in vitro* model for drug absorption and transport due to its wide application. Caco-2 cell line was derived from a human colorectal carcinoma and could form a cell monolayer with morphological and functional similarities to the human small intestinal epithelium. Not only the cells formed tight intercellular junctions similar to those of human intestinal epithelium, but also they expressed ATP-binding cassette (ABC) membrane transporters such as P-glycoprotein (P-gp) and multidrug resistance protein (MRP) (Li et al., 2012). In this study, aloe-emodin, rhein, emodin, and chrysophanol were the representative active ingredients of rhabarb, and their absorption properties and mechanisms in different environments were investigated. The effect of multi-herb prescription on absorption characteristics of representative components was studied.

2. Materials and methods

2.1. Absorption characteristics *in situ* model

2.1.1. Preparation of working perfusate

Shenkang Injection (Xi'an Shiji Shengkang Pharmaceutical Industry Co., Ltd., Xi'an, China) was concentrated to obtain Shenkang extract (SKE) with a relative density of 1.22 at 60 °C. The content of aloe-emodin, rhein, emodin and chrysophanol in SKE was (202.93 ± 10.35), (438.53 ± 7.45), (263.80 ± 7.95), and (41.90 ± 3.75) µg/g, respectively. The SKE intestinal perfusion solution was freshly prepared from a Krebs-Ringer (K-R) (containing 7.8 g/L NaCl, 0.35 g/L KCl, 0.37 g/L CaCl₂, 1.37 g/L NaHCO₃, 0.32 g/L NaH₂PO₄, 0.02 g/L MgCl₂, and 1.4 g/L glucose) solution containing 22.50 mg/mL of SKE. The final concentrations of aloe-emodin, rhein, emodin and chrysophanol in SKE perfusate were 4.57, 9.87, 5.94 and 0.94 µg/mL, respectively.

Aloe-emodin, rhein, emodin and chrysophanol (National Institutes for Food and Drug Control, Beijing, China) were firstly dissolved in dimethylsulfoxide (DMSO) and then diluted with a fresh K-R solution to obtain the intestinal perfusion solution of rhabarb anthraquinone ingredients (RAI). The final concentration of DMSO in RAI perfusate was below 1.0% to ensure the safety to the small intestine. The concentrations of aloe-emodin, rhein, emodin and chrysophanol in RAI perfusate were the same as those in SKE perfusate.

2.1.2. Single-pass intestinal perfusion in rats

Male Sprague-Dawley rats [body weight: (250 ± 50) g] were purchased from Medical Laboratory Animals Center of Xi'an Jiaotong University. All animal procedures were performed according

to the research protocol approved by the Laboratory Animal Care Committee of Xi'an Jiaotong University (No. XJTULAC2017-403).

The rats were raised in a controlled environment with a temperature of (23–26) °C and a relative humidity of 40%–60%. Light and dark cycles were matched to the rats' natural circadian rhythms for at least one week to facilitate their adaptation to the housing conditions. The rats were fasted overnight with free access to water before the experiment. Rats were anesthetized and then placed on warm panel to maintain normal body temperature during surgery. A midline incision was made in the abdomen. The small intestine segment, approximately 10 cm of duodenum, jejunum and colon, was exposed. Incisions were made at both ends of the segment for the inflow and outflow perfusate. Cannulas were inserted at the inlet and outlet of segments and secured by ligation. The exposed segments were placed back into the peritoneal cavity and the cavity was covered by saline-soaked gauze. The feeding end was connected to the peristaltic pump (BT-100, Shanghai Qingpu Huxi Instrument Factory, Shanghai, China) and gently flushed using pre-warmed saline (37 °C) to remove intestinal contents.

The SKE or RAI perfusate was firstly infused at a flow rate of 1 mL/min for 5 min and then at a flow rate of 0.2 mL/min for 30 min for absorption equilibrium. A certain volume SKE or RAI perfusate was placed into a known-weight glass tube and infused at a constant flow rate of 0.2 mL/min. Samples from the outflow end were collected to a new weighed glass tube at 15-min intervals up to 120 min. The collected samples and remaining perfusion solution were weighed. An aliquot of 0.5 mL perfusate or collected sample was spiked to weigh for gain the density (ρ) of the inflow and outflow of perfusate. The contents of aloe-emodin, rhein, emodin and chrysophanol in the collected samples were analyzed by HPLC. At the end of the experiment, the animals were euthanized. The tested intestinal segments were cut off and placed in saline without any stretch or crimp. The length (L) and width ($2\pi r$, r is the radius of intestinal lumen) of the segments were measured.

2.1.3. HPLC determination

The collected samples from SKE or RAI perfusate (400 µL) were transferred into polypropylene tubes and 2 mol/L hydrochloric acid solution (200 µL) and 800 µL of acetonitrile were added in turn, then the mixture was vortexed vigorously for 2 min, followed by centrifugation at 12 000 r/min for 10 min. The supernatant was collected for HPLC analysis. The HPLC system (LC-2010HT Shimadzu, Kyoto, Japan) consisted of a LC-20AB pump, a SPD-M20A UV detector, a Diamonsil C₁₈ column (150 mm × 4.6 mm, 5 µm, Dikma Technologies, Beijing China). The mobile phase was composed of acetonitrile (A) and 0.1% phosphoric acid solution (B), running at a flow rate of 1.0 mL/min. The column was eluted using a gradient: 30%–35% A (0–5 min), 35%–40% A (5–10 min), 40%–46% A (10–16 min) and 46%–90% A (16–30 min) at 30 °C. aloe-emodin, rhein, emodin and chrysophanol were detected at 254 nm.

2.1.4. Data analysis

Gravimetric method was used to revise the volume change in perfusion solution due to intestinal segments absorbing moisture

during perfusion. The volume of inflow perfusate (Q_{in} , mL) and outflow solution (Q_{out} , mL) was revised as given by Eqs. (1) and (2), respectively.

$$Q_{in} = \frac{M_{in}}{\rho_{in}} \quad (1)$$

$$Q_{out} = \frac{M_{out}}{\rho_{out}} \quad (2)$$

where M_{in} and M_{out} (g) were the mass of the inflow and outflow perfusate, respectively, ρ_{in} and ρ_{out} (g/mL) were the density of the inflow and outflow perfusate, respectively.

The effective permeability coefficient (P_{eff}) was calculated as the following equations.

$$P_{eff} = \frac{-Q \times \ln \frac{C_{out} \times Q_{out}}{C_{in} \times Q_{in}}}{2\pi L} \quad (3)$$

where Q (mL/min) was the flow rate of perfusate through the intestinal, C_{in} and C_{out} ($\mu\text{g/mL}$) were the concentration of drug at the inflow and outflow perfusate, respectively.

2.2. Absorption characteristics in vitro model

2.2.1. Bidirectional transport of SKE and RAI in Caco-2 cell monolayer model

Caco-2 cells were obtained from the CHI Scientific Ltd. (Jiangyin, China) and were plated into 12-well Millicell[®] hanging cell insert (0.4 μm pore size, Millipore, Billerica, USA) at a density of (1×10^5)/ cm^2 . Cells were cultured in DMEM (Hyclone, USA supplemented with 10% fetal bovine serum (Gibco Life Technologies, Grand Island, USA) and antibiotics (100 U/mL penicillin and 100 U/mL streptomycin) in a humidified incubator at 5% CO_2 about 20 d. Transepithelial electrical resistance (TEER) was measured by a Millicell[®] ERS meter (Millipore, Billerica, USA) till its values were above 500 $\Omega \cdot \text{cm}^2$.

The cells were rinsed with warm HBSS (37 $^\circ\text{C}$) and allowed to equilibrate for 15 min. For assessment the transport characteristics from apical (AP) to basolateral (BL) side (AP-BL), 0.5 mL of HBSS containing 0.025, 0.05 and 0.1 mg/mL of SKE was added to AP and 1.5 mL of HBSS was added to BL. Cells were maintained at 37 $^\circ\text{C}$ with orbital shaking at 50 r/min. At pre-determined intervals, 1.0 mL of transport buffer at BL was collected and an equal amount of fresh HBSS was instantly added. For BL-AP experiments, 1.5 mL of HBSS containing different concentrations of SKE was added to BL and 0.5 mL of HBSS was added to AP. And 0.3 mL of transport buffer at AP was collected and an equal amount of fresh HBSS was instantly added. RAI solutions were freshly prepared in DMSO-HBSS solution and the final DMSO concentration in mixture solution was below 0.5%. The contents of aloë-emodin, rhein, emodin and chrysophanol in RAI were calculated according to their contents in 0.025, 0.05 and 0.1 mg/mL SKE. The collected transport buffer was dried in a low temperature vacuum and residue was re-dissolved with methanol. The contents of aloë-emodin, rhein, emodin and chrysophanol were assessed using HPLC method as described above.

2.2.2. Effects of verapamil and MK-571 on SKE transport

To investigate the potential role of transport proteins on the bidirectional transport characteristics of rhuëarb anthraquinone, verapamil and MK-571 (Sigma-Aldrich St. Louis, USA), as a P-gp and a MRP inhibitor, respectively, were added to HBSS solution containing 0.1 mg/mL of SKE. The concentrations of verapamil and MK-571 in this SKE-HBSS solution were both 100 $\mu\text{mol/L}$ (Chen et al., 2016).

2.2.3. Data analysis

The cumulative transport mass (M , μg) was calculated using the equation (4). The apparent permeability (P_{app}) used as an expression of the transport rate constant was calculated as equation (5):

$$M = C_i \times V + \sum C_{i-1} \times V_t \quad (4)$$

$$P_{app} = \frac{dC}{dt} \frac{V}{A \times C_0} \quad (5)$$

where V (mL) was the volume of the solution in transport chamber, V_t (mL) was the volume of collected sample at different time, C_i ($\mu\text{g/mL}$) was the drug concentration of collected transport buffer at different time. dC/dt was the slope of the linear regression of drug concentration with time, A was the area of the insert membrane in cm^2 , and C_0 ($\mu\text{g/mL}$) was the initial concentration in donor chamber.

Efflux ratio (ER) was calculated from equation (6):

$$ER = \frac{P_{app_{B-A}}}{P_{app_{A-B}}} \quad (6)$$

2.2.4. Statistical analysis

Results were expressed as mean \pm standard deviation (S.D.) for all experiments. An analysis of variance (ANOVA) test was used to determine the statistical significance of differences between groups. The statistical significance for the differences of the means was determined using t -test and $P < 0.05$ was considered statistically significant.

3. Results and discussion

3.1. HPLC analysis

Aloë-emodin, rhein, emodin and chrysophanol from both collected perfusates and cell transport buffers can be well isolated and detected by HPLC. The standard curves between the peak area of four ingredients and their concentration were evaluated by least squares regression analysis. Standard curves were linear ($r = 0.99$ 94–0.9999) over the ranges 0.25–70.60 $\mu\text{g/mL}$ in collected perfusates and 0.05–50.00 $\mu\text{g/mL}$ in cell transport buffers. The repeatability, precision and accuracy were assessed by analyzing quality control samples at three concentrations in five duplicates. The repeatability and precision, expressed as coefficient of variation (%CV), were $< 2.4\%$ and 5.1% for collected perfusates, 5.0% and 7.7% for cell transport buffers, respectively. The accuracy (expressed as recovery) ranged from 95.7% to 105.7% for collected perfusates and from 95.2% to 105.3% for cell transport buffers, respectively. These ingredients were found to be stable in collected perfusates and cell transport buffers after storage for at least 4 h at room temperature, and at least two weeks after treatment at -20 $^\circ\text{C}$.

3.2. Absorption characteristics of SKE and RAI in situ

The absorption characteristics of aloë-emodin, rhein, emodin and chrysophanol in rat different intestinal segments, (Abuהלwa, Foster, & Upton, 2016) expressed as P_{eff} , were illustrated in Fig. 2. For SKE, the duodenum and colon absorbed the most aloë-emodin compared to jejunum. There was the highest absorption coefficient in duodenum, a high absorption coefficient in jejunum and a low absorption coefficient in colon for rhein ($P < 0.05$). The P_{eff} value of emodin in duodenum was significantly higher than that in jejunum and colon ($P < 0.05$). The colon displayed a high level of absorption for chrysophanol and its P_{eff} value was obviously different in duodenum, jejunum and colon ($P < 0.05$) (Fig. 2A). As shown in Fig. 2B, the easily absorbed intestinal seg-

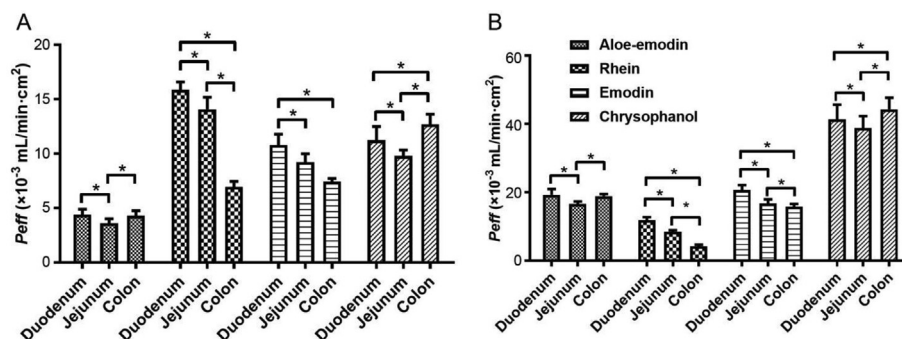


Fig. 2. P_{eff} of aloe-emodin, rhein, emodin and chrysophanol in SKE (A) and RAI (B) in rat different intestinal segments (mean \pm SD, $n = 5$, $*P < 0.05$).

ments of aloe-emodin, rhein, emodin and chrysophanol in RAI were consistent with those in SKE. There was the high level absorption in duodenum for aloe-emodin, rhein and emodin, and the high level absorption in colon for chrysophanol. It might be due to the different pK_a values (pK_a : 4.72 for rhein, 8.64 for aloe-emodin, 5.70 for emodin and 8.58 for chrysophanol) (Wang, Yang, & Song, 2001) of these four ingredients, belonging to acidic or weak acidic drug, leading to selective intestinal absorbed. As some studies have reported that luminal pH may significantly influence the drug absorption of oral administration, especially for weakly acidic and weakly basic drugs (Dubbelboer, Dahlgren, Sjögren, & Lennernäs, 2019).

For the same tested intestinal segment, the P_{eff} values of aloe-emodin, emodin and chrysophanol in RAI were higher than those in SKE, however, this value of rhein in RAI was lower than that in SKE. It can be inferred that co-existing factors had profound influences on the intestinal absorption of active ingredients. For aloe-emodin, emodin and chrysophanol, their pK_a values were close to the intestinal physiological conditions, which allowed them to remain more molecular form in intestine. It was possible that the other ingredients in SKE may serve to interfere with the absorption of these three ingredients in association with the reduction of P_{eff} values. However, rhein had a low pK_a values and dissociated in the intestinal physiological conditions. If the co-existing ingredients contribute to the dissociation equilibrium shifting towards the molecular form, this may be likely to increase intestinal absorption of rhein. Some researches on drug compatibility mechanisms have shown that the intestinal absorptions of active ingredients were improved or decreased when they were co-administered (Huang et al., 2016; Li et al., 2018).

3.3. Absorption characteristics of SKE and RAI in vitro

The cumulative transport mass over time course from AP to BL was illustrated in Fig. 3 for aloe-emodin, rhein, emodin and chrysophanol in different concentration SKE. Among the testing time plot, the transport mass of four rhubarb anthraquinone compounds increased with time. And with increasing concentration, their cumulative transport mass also increased. The transport mass of four rhubarb anthraquinone compounds in RAI exhibited similar trend (Results not given). These results suggested that the cumulative transport of aloe-emodin, rhein, emodin and chrysophanol was time- and concentration-dependent (Oga, Sekine, Shitara, & Horie, 2012; Zeng et al., 2017).

The two-way transport properties of four rhubarb anthraquinone compounds in different concentrations SKE and RAI, expressed as $P_{app(A-B)}$ and $P_{app(B-A)}$, were summarized Table 1. The $P_{app(A-B)}$ values of aloe-emodin were similar in 0.025 and 0.05 mg/mL SKE and slightly decreased in 0.1 mg/mL SKE, and the values were not significant different ($P > 0.05$). For transport

for BL to AP, the $P_{app(B-A)}$ values of aloe-emodin in 0.025 and 0.05 mg/mL SKE were obviously higher than that in 0.1 mg/mL SKE ($P < 0.05$). And the $P_{app(B-A)}$ values were higher than the $P_{app(A-B)}$ values for aloe-emodin in all concentration SKE, resulting in ER values greater than 1. The $P_{app(A-B)}$ and $P_{app(B-A)}$ values of aloe-emodin in different concentration RAI showed the similar trend to SKE. These data inferred that the cell transport of aloe-emodin may be mainly passive transport involving carrier-mediated or efflux protein-mediated transport (Bonetti et al., 2018).

For rhein, the $P_{app(A-B)}$ and $P_{app(B-A)}$ values did not show a concentration dependence. But the $P_{app(A-B)}$ values were higher than $P_{app(B-A)}$ values, especially, the formers were 1.4- and 1.6-fold of the latters for 0.025 and 0.05 mg/mL SKE, respectively ($P < 0.05$). It was found that all $P_{app(A-B)}$ values of rhein were higher than $P_{app(B-A)}$ values for both SKE and RAI. It suggested that rhein was mainly passively transported across Caco-2 cell monolayer (Zhou et al., 2012).

For emodin and chrysophanol in different concentration SKE, $P_{app(B-A)}$ values were all significantly higher than $P_{app(A-B)}$ values ($P < 0.05$). Corresponding ER s were 1.60–1.46 for emodin and 2.22–1.61 for chrysophanol, respectively. The same trends were found in different concentration RAI. It was inferred that emodin and chrysophanol may be substrates for ATP-binding cassette membrane transporters. In addition, for high concentration SKE, the $P_{app(B-A)}$ values of emodin and chrysophanol were significantly lower than those in low and middle concentration SKE, which may be due to the combination effect of an added transport from AP to BL caused by concentration gradient effect and a reduced transport from BL to AP caused by limited transport carrier number (Chen et al., 2014).

Further, transport characteristics of four rhubarb anthraquinone compounds in SKE and RAI were compared to observe whether the absorption of these ingredients was influenced by different situation. As shown in Table 1, the $P_{app(A-B)}$ and $P_{app(B-A)}$ values of aloe-emodin in RAI were all less than those in SKE, indicating that aloe-emodin has higher cumulative transport in SKE. However, for rhein, emodin and chrysophanol, the $P_{app(A-B)}$ and $P_{app(B-A)}$ values in RAI were all higher than those in SKE, which suggested their transport rates in RAI were high. ER is one of the important indicators to speculate transport mechanism. It was found that the ER of aloe-emodin ranged from 1.07 to 1.32, 1.10 to 1.22, respectively, was similar between RAI and SKE. Rhein's ER s in RAI and SKE were all close to and lower than 1.0. The ER s of emodin and chrysophanol in RAI and SKE were all close to or above 1.5. These data suggested that four rhubarb anthraquinone compounds in SKE had similar absorption mechanism as them in RAI although they exhibited different transport behavior in SKE and RAI (Zheng, Zhou, Wan, Chen, & He, 2015).

P-gp and MRP are known to be responsible for the efflux of drug from the cell, therefore, one P-gp inhibitor (verapamil) and one

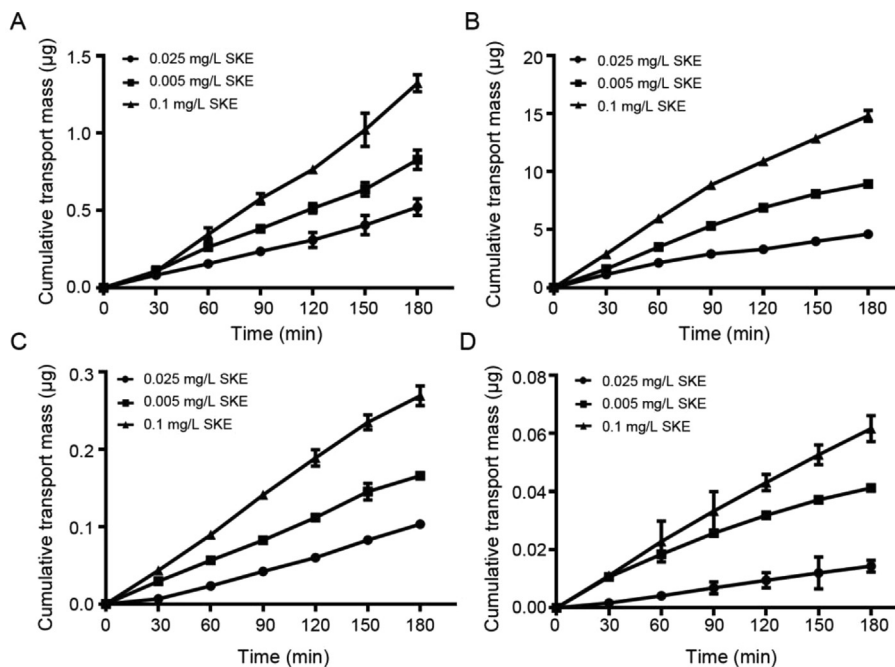


Fig. 3. Cumulative transport mass (AP-BL) over time course of aloe-emodin (A), rhein (B), emodin (C) and chrysophanol (D) in SKE (mean ± SD, n = 3).

Table 1

Papp (×10⁻⁶ cm/s) and *ER* of four rhubarb anthraquinone compounds in different concentration SKE and RAI (mean ± SD, n = 3).

Index ingredients	Concentrations (mg/mL)	SKE			RAI		
		<i>Papp</i> _(A-B)	<i>Papp</i> _(B-A)	<i>ER</i>	<i>Papp</i> _(A-B)	<i>Papp</i> _(B-A)	<i>ER</i>
Aloe-emodin	0.025	19.64 ± 2.04	23.96 ± 0.59 ^c	1.22	10.59 ± 1.21	14.01 ± 1.77	1.32
	0.05	19.41 ± 1.47	23.36 ± 1.56 ^c	1.20	15.08 ± 1.54 ^a	16.14 ± 1.83	1.07
	0.1	17.61 ± 0.74	19.40 ± 1.65 ^{a, b}	1.10	14.26 ± 1.06 ^a	17.26 ± 0.79 ^{a, c}	1.21
Rhein	0.025	27.43 ± 1.47	20.98 ± 0.40	0.96	30.30 ± 0.95	31.21 ± 0.55	1.03
	0.05	28.02 ± 0.14	20.48 ± 0.46 ^c	0.73	35.04 ± 1.72 ^a	26.63 ± 1.031 ^c	0.76
	0.1	31.00 ± 2.31	19.83 ± 0.37 ^c	0.64	34.20 ± 1.13 ^a	30.10 ± 1.371 ^c	0.88
Emodin	0.025	7.40 ± 0.08	11.88 ± 1.11 ^c	1.60	8.21 ± 0.73	12.40 ± 0.42	1.51
	0.05	6.65 ± 0.16 ^a	10.55 ± 0.31 ^c	1.59	7.74 ± 0.61	11.46 ± 0.27	1.48
	0.1	6.24 ± 0.29 ^a	9.13 ± 0.42 ^{a, b, c}	1.46	7.31 ± 0.97	11.85 ± 0.66	1.62
Chrysophanol	0.025	6.23 ± 0.86	13.85 ± 0.65 ^c	2.22	8.42 ± 1.11	17.43 ± 0.85	2.07
	0.05	6.87 ± 0.23	13.87 ± 0.86 ^c	2.02	8.99 ± 0.44	15.73 ± 1.05	1.75
	0.1	6.63 ± 0.48	10.67 ± 0.15 ^{a, b, c}	1.61	7.97 ± 1.06	13.23 ± 0.67	1.66

Note: ^a compared with low-concentration (0.025 mg/mL) *P* < 0.05, ^b compared with middle concentration (0.05 mg/mL) *P* < 0.05, ^c AP side compared with BL side *P* < 0.05.

MRP inhibitor (MK571) (Zhu et al., 2013) were used to test the possible role of efflux protein on the absorption of four rhubarb anthraquinone compounds in SKE, and the result was examined in Fig. 4. After addition of verapamil and MK571, *ER* values of rhein were similar to the SKE group (0.1 mg/mL SKE). This was in line with previous data obtained by two-way transport properties of rhein inferring a passive transport mechanism. While, *ER* values of aloe-emodin, emodin and chrysophanol were all decreased, among which, the verapamil groups in aloe-emodin and emodin reduced the most, and the MK571 group in chrysophanol reduced the most (*P* < 0.05). Therefore, aloe-emodin, emodin and chrysophanol might be substrates for P-gp and MRP, and aloe-emodin and emodin were more susceptible to P-gp, while, chrysophanol was mainly affected by MRP.

4. Conclusion

Multi-herb prescription is recognized as a main pattern of TCM, in which active ingredients interact with each other and may have influences on their pharmacokinetics and pharmacodynamics. In this study, it was inferred that the complex coexistence environ-

ment of ingredients and microenvironments of different study models may affect the absorption behavior of Rhubarb anthraquinone ingredients but not their absorption mechanism through *in situ* and *in vitro* experiments. These results provide insight into the absorption characteristics of the active ingredients in multi-

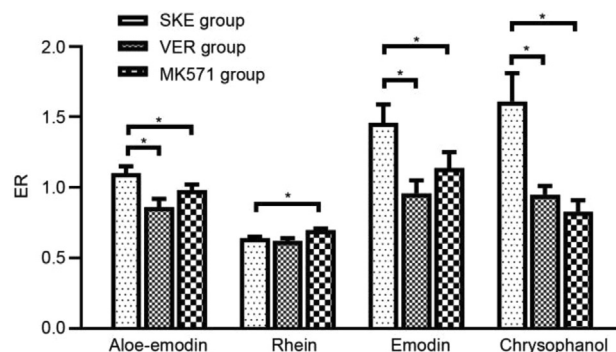


Fig. 4. Effects of VER and MK-571 on two-way transport of aloe-emodin, rhein, emodin and chrysophanol in SKE (mean ± SD, n = 3, **P* < 0.05).

herb prescription, with an expectation to elucidate the influence of TCM interactions.

Declaration of Competing Interest

The authors declare that they have no known competing financial interests or personal relationships that could have appeared to influence the work reported in this paper.

Acknowledgements

The authors thank Xi'an ShijiShengkang Pharmaceutical Industry Co. Ltd. for providing Shengkang Injection for this study. This work was supported by the National Natural Science Foundation of China (No. 81673397) and the Natural Science Basic Research Plan in Shaanxi Province of China (No. 2020JM-023).

References

- Abuhelwa, A. Y., Foster, D. J. R., & Upton, R. N. (2016). A quantitative review and meta-models of the variability and factors affecting oral drug absorption—Part ii: Gastrointestinal transit time. *The AAPS Journal*, *18*(5), 1322–1333.
- Bonetti, J., Zhou, Y., Parent, M., Clarot, I., Yu, H., Fries-Raeth, L., ... Gaucher, C. (2018). Intestinal absorption of S-nitrosothiols: Permeability and transport mechanisms. *Biochemical Pharmacology*, *155*, 21–31.
- Chen, L., Lu, X., Liang, X., Hong, D., Guan, Z., Guan, Y., & Zhu, W. (2016). Mechanistic studies of the transport of peimine in the Caco-2 cell model. *Acta Pharmaceutica Sinica B*, *6*(2), 125–131.
- Chen, Y., Wang, Y., Zhou, J., Gao, X., Qu, D., & Liu, C. (2014). Study on the mechanism of intestinal absorption of epimedins a, b and c in the Caco-2 cell model. *Molecules (Basel, Switzerland)*, *19*(1), 686–698.
- Dubbelboer, I. R., Dahlgren, D., Sjögren, E., & Lennernäs, H. (2019). Rat intestinal drug permeability: A status report and summary of repeated determinations. *European Journal of Pharmaceutics and Biopharmaceutics*, *142*, 364–376.
- Huang, J., Zhang, J., Bai, J., Xu, W., Wu, D., & Qiu, X. (2016). LC-MS/MS determination and interaction of the main components from the traditional Chinese drug pair Danshen-Sanqi based on rat intestinal absorption. *Biomedical Chromatograph*, *30*(12), 1928–1934.
- Li, Q., Yang, Y., Zhou, T., Wang, R., Li, N., Zheng, M., ... Ma, B. L. (2018). A composite strategy to study the pharmacokinetics of TCMS: Taking *Coptidis Rhizoma*, and *Coptidis Rhizoma-Glycyrrhizae Radix* et *Rhizoma* as examples. *Molecules*, *23*(8), 2042.
- Li, C., Zhang, L., Zhou, L., Wo, S. K., Lin, G., & Zuo, Z. (2012). Comparison of intestinal absorption and disposition of structurally similar bioactive flavones in *Radix Scutellariae*. *The AAPS Journal*, *14*(1), 23–34.
- Lian, J. P., Han, S., Fang, Z. Y., Li, X. C., & Zuo, Y. (2015). Effects of Shengkang Injection on chronic renal failure: A Meta-analysis. *Chinese Traditional Patent Medicine*, *37*(8), 1677–1682.
- Lin, Q., Ling, L. Q., Guo, L., Gong, T., Sun, X., & Zhang, Z. R. (2015). Intestinal absorption characteristics of imperialine: *In vitro* and *in situ* assessments. *Acta Pharmaceutologica Sinica*, *36*(7), 863–873.
- Oga, E. F., Sekine, S., Shitara, Y., & Horie, T. (2012). P-glycoprotein mediated efflux in Caco-2 cell monolayers: The influence of herbals on digoxin transport. *Journal of Ethnopharmacology*, *144*(3), 612–617.
- Wang, D., Yang, G., & Song, X. (2001). Determination of pKa values of anthraquinone compounds by capillary electrophoresis. *Electrophoresis*, *22*(3), 464–469.
- Yang, H., Hao, Q., Cheng, J., Wang, M., Zou, J., Zhang, X., & Guo, D. (2020). Exploring the compatibility mechanism of ShengDiHuang Decoction based on the *in situ* single-pass intestinal perfusion model. *Biopharmaceutics & Drug Disposition*, *41*(1–2), 44–53.
- Ying, P., Min, F., Chong, S. P., Meng, Y. W., & Xiao, B. L. (2018). Alleviating the intestinal absorption of rhein in rhubarb through herb compatibility in Tiaowei Chengqi Tang in Caco-2 cells. *Evidence-Based Complementary and Alternative Medicine*, *3*, 593.
- Zeng, Z., Shen, Z. L., Zhai, S., Xu, J. L., Liang, H., Shen, Q., & Li, Q. Y. (2017). Transport of curcumin derivatives in Caco-2 cell monolayers. *European Journal of Pharmaceutics and Biopharmaceutics*, *117*, 123–131.
- Zhang, Z. H., Li, M. H., Liu, D., Chen, H., Chen, D. Q., Tan, N. H., ... Zhao, Y. Y. (2018). Rhubarb protect against tubulointerstitial fibrosis by inhibiting TGF- β /smad pathway and improving abnormal metabolome in chronic kidney disease. *Frontiers in Pharmacology*, *9*, 1029.
- Zhang, Y. F., Sun, J. X., Liu, H., & Zhai, X. L. (2017). Effects of injection Shengkang and alprostadil combination on contrast-induced nephropathy in patient with diabetes complicated with mild to moderate renal insufficiency. *Bangladesh Journal of Pharmacology*, *12*(3), 308–312.
- Zhang, Z. H., Vaziri, N. D., Wei, F., Cheng, X. L., Bai, X., & Zhao, Y. Y. (2016). An integrated lipidomics and metabolomics reveal nephroprotective effect and biochemical mechanism of *Rheum officinale* in chronic renal failure. *Scientific Reports*, *6*, 22151.
- Zheng, M., Zhou, H., Wan, H., Chen, Y. L., & He, Y. (2015). Effects of herbal drugs in Mahuang decoction and their main components on intestinal transport characteristics of ephedra alkaloids evaluated by a Caco-2 cell monolayer model. *Journal of Ethnopharmacology*, *164*, 22–29.
- Zhou, W., Di, L. Q., Wang, J., Shan, J. J., Liu, S. J., Ju, W. Z., & Cai, B. C. (2012). Intestinal absorption of forsythoside A in *in situ* single-pass intestinal perfusion and *in vitro* Caco-2 cell models. *Acta Pharmaceutologica Sinica*, *33*(8), 1069–1079.
- Zhu, M. L., Liang, X. L., Zhao, L. J., Liao, Z. G., Zhao, G. W., Cao, Y. C., ... Luo, Y. (2013). Elucidation of the transport mechanism of baicalin and the influence of a *Radix Angelicae Dahuricae* extract on the absorption of baicalin in a Caco-2 cell monolayer model. *Journal of Ethnopharmacology*, *150*(2), 553–559.